Numerical simulation of the flow of wet granular materials

S. Khamseh, J.-N. Roux and F. Chevoir

. Université Paris-Est, Laboratoire Navier, 2 allée Kepler, Cité Descartes, 77420 Champs-sur-Marne, France

Résumé :

Nous étudions par simulation numérique discrète (DEM) le comportement d'assemblages de billes sphériques en écoulement de cisaillement à contrainte normale P contrôlée, en présence de forces capillaires créées par une faible quantité de fluide intertitiel, sous forme de ménisques joignant les grains voisins (état pendulaire). Nous portons une attention particulière à l'approche de la limite quasi-statique et caractérisons le comportement du matériau en exprimant le coefficient de frottement interne et la densité en fonction de deux paramèters de contrôle sans dimension, le nombre d'inertie I et la pression réduite P (qui compare les forces de confinement et la résistance à la traction d'un ménisque). Les forces capillaires ont un effet notable sur la rhéologie jusqu'à des valeurs de P* de plusieurs unités, particulièrement dans le cas de force attractives à plus longue portée, pour les volumes de ménisques plus importants. Cet effet est relié à l'anisotropie de la texture du réseau des contacts et des interactions à courte distance.*

Abstract :

We use a DEM method to simulate dense assemblies of frictional spherical grains in 3D steady shear flow under controlled normal stress P, either dry or in the presence of a small amount of an interstitial liquid, which gives rise to capillary menisci and attractive forces. We pay special attention to the quasi-static limit of slow flow. The system behavior is characterized by the dependence of internal friction coefficient and solid fraction on two dimensionless control parameters : the inertial number, I and the reduced pressure, P, comparing confining forces to contact tensile strength. Capillary forces have a significant effect on the macroscopic behavior of the system, up to P* values of several unities, especially for longer force ranges associated with larger menisci. We relate this effect to fabric anisotropy parameters of contact and distant interactions.*

Mots clefs : **Granular material ; Wet grains ; Capillary force**

1 Introduction

Significant recent progress in the understanding of the rheology of granular materials in dense flows has recently been gained from the consideration steady shear flows [1, 2, 3], under constant normal stress P. Constitutive relations are then conveniently written for internal friction μ^* and solid fraction ϕ, as functions of an adequate reduced form of shear rate $\dot{\gamma}$, the inertial number $I = \dot{\gamma}\sqrt{\frac{m}{aP}}$ (m and a denoting particle mass and diameter). If cohesion is introduced, another dimensionless control parameter should be introduces [4, 5] : the reduced pressure P^* is defined as the ratio $P^* = \frac{Pa^2}{F_0}$ of applied pressure P on grains with diameter a to tensile strength of cohesive contacts, force F_0.

We report here on simulations of spherical grain assemblies in which cohesion stem from capillary forces acting in the narrow gaps between neighboring grains, where menisci of a wetting fluid are formed.

2 Model and Simulation

We simulate homogeneous Couette flows, as a uniform shear rate $\dot{\gamma} = dv_x/dy$ is imposed to mono-sized spherical grain assemblies. We use periodic, Lees-Edwards boundary conditions (no wall), and the cell height H (in the y direction) is allowed to fluctuate to keep normal stress $\sigma_{yy} = P$ constant [2, 3, 5]. Particles interact via Hertz-Mindlin elasticity and Coulomb friction (with coefficient $\mu = 0.3$) in their contacts as in [6], supplemented by the Maugis force [7] for capillary attraction (inter-particle distance D, meniscus volume V and surface tension Γ) assuming complete wetting :

$$F^{cap.} = \pi a \Gamma [1 - \frac{1}{\sqrt{1 + \frac{4V}{\pi a D^2}}}] \tag{1}$$

The present study is limited to the pendular state (small saturation) [8]. The liquid is confined within (constant volume) menisci joining neighboring grains, which form as soon as two particles touch [10] and disappear once the inter-particle distance exceeds the rupture distance, $D_0 = V^{1/3}$. Macroscopic properties were shown not to be sensitive to assumptions about meniscus volumes [9] in such models. Capillary forces $F^{cap.}$, for solid contacts ($h \leq 0$) stay equal to $F_0 = \pi a \Gamma$.

Elastic properties are such that contact deflections are kept very small (rigid particle limit [3]). By definition $I \to 0$ corresponds to the quasistatic limit. Our simulations investigate the interval $10^{-3} < I < 10^{-0.5}$, while P^* values range from infinity (no cohesion) down to 0.43 (corresponding, e.g., to $a = 1\mu m, P = 100kPa$ and $\Gamma = 73mJ.m^{-2}$, the surface tension of water). $V/a^3 = 10^{-3}$ (thus setting D_0/a to 0.1) used in our simulations, corresponds to saturations slightly below 1%.

3 Macroscopic observations

Macroscopic friction coefficient μ^* (Fig. 1a), measured as a time average of the ratio of the shear stress to the normal stress ($\mu^* =< \frac{|\sigma_{12}|}{\sigma_{22}} >$), is recorded along with solid fraction ϕ (Fig. 1b) for different values of I and P^*. As I decreases and the quasistatic limit of $I \to 0$ is approached, μ^* decreases to $\mu_0^*(P^*)$ and ϕ increases to $\phi_0(P^*)$, characterizing quasistatic plastic flow.

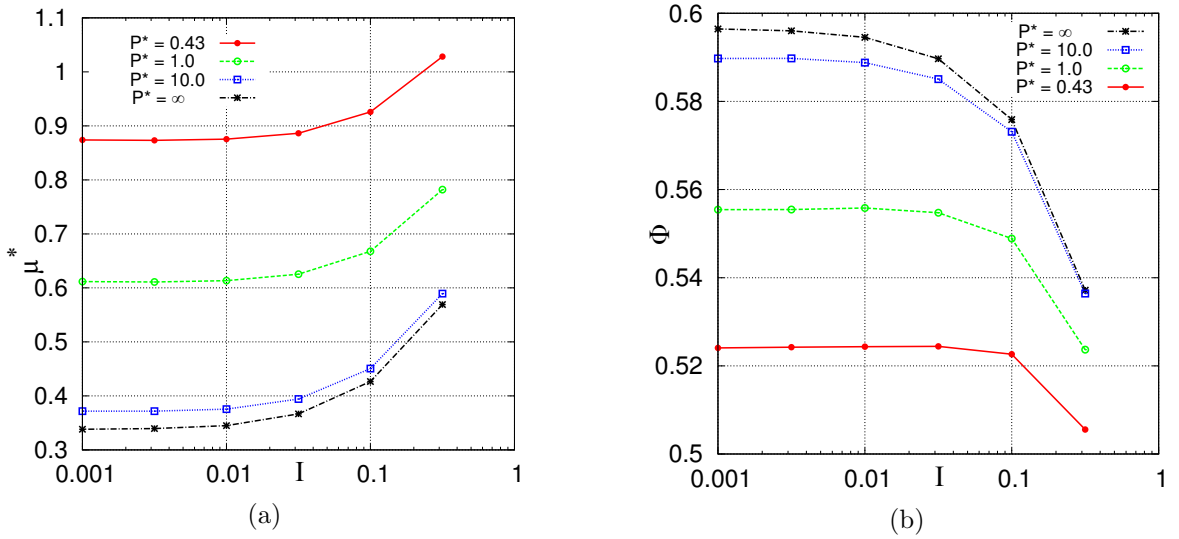

FIGURE 1 – Macroscopic friction coefficient μ^* (a) and solid fraction ϕ (b) versus inertial number I for different values of reduced pressure P^* when rupture distance of meniscus is $D_0/a = 0.1$.

If $(\phi_0 - \phi) \propto I^\nu$ as I tends to zero, this corresponds to a divergence of effective viscosity in constant density shear flow as $(\phi_0 - \phi)^{-1/\nu}$ (in the range 0.4 - 0.5 in our results).

While qualitatively similar results were observed in cohesionless and cohesive systems [5], the effect of capillary forces on the system behavior is considerably stronger in the present case, as μ^* increases from about 0.35 to more than 0.6 between P^* infinite and $P^* = 1$.

This is due, to some extent, to the longer attraction range (here $D_0/a = 0.1$), compared to previous 2D results [5], as confirmed by Fig. 2 : the increase of internal friction and the decrease of density caused by cohesion are reduced for smaller D_0.

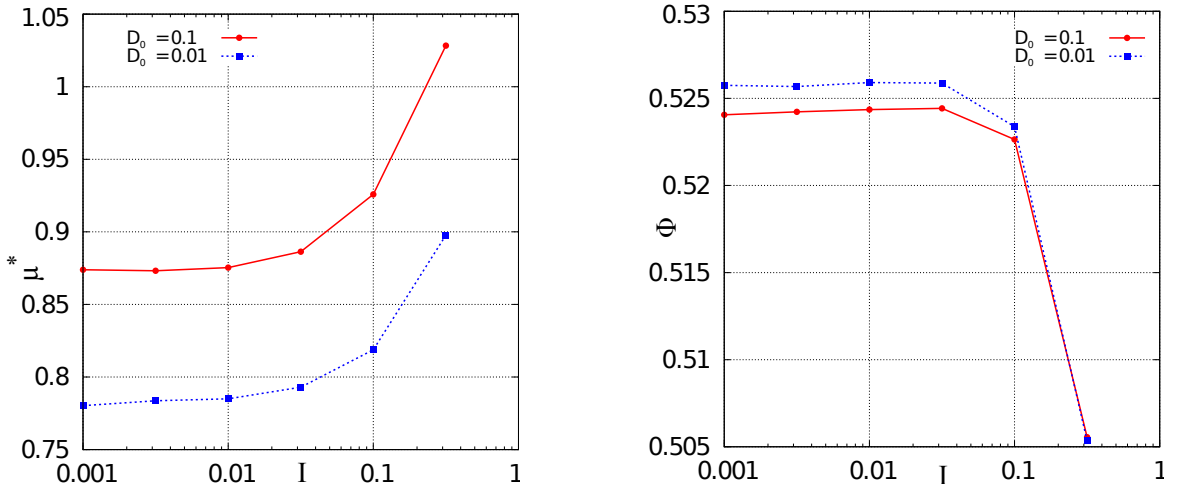

(a) (b)

FIGURE 2 – Macroscopic friction coefficient μ^* (a) and solid fraction ϕ (b) versus inertial number I with $P^* = 0.43$ for two different values of rupture distances 0.1 (red circle points) and 0.01 (blue squares).

To understand the microscopic origin of such rheological features, we now investigate properties of contact networks and forces.

4 Microscopic observations

4.1 Coordination numbers

The coordination number of all interacting pairs z, can be written as $z = z_c + z_d$ with z_c the average number of contacts per grain and z_d that of distant interactions through the liquid bridges. z and z_c are plotted for different values of I and P^* in Fig. 3a.

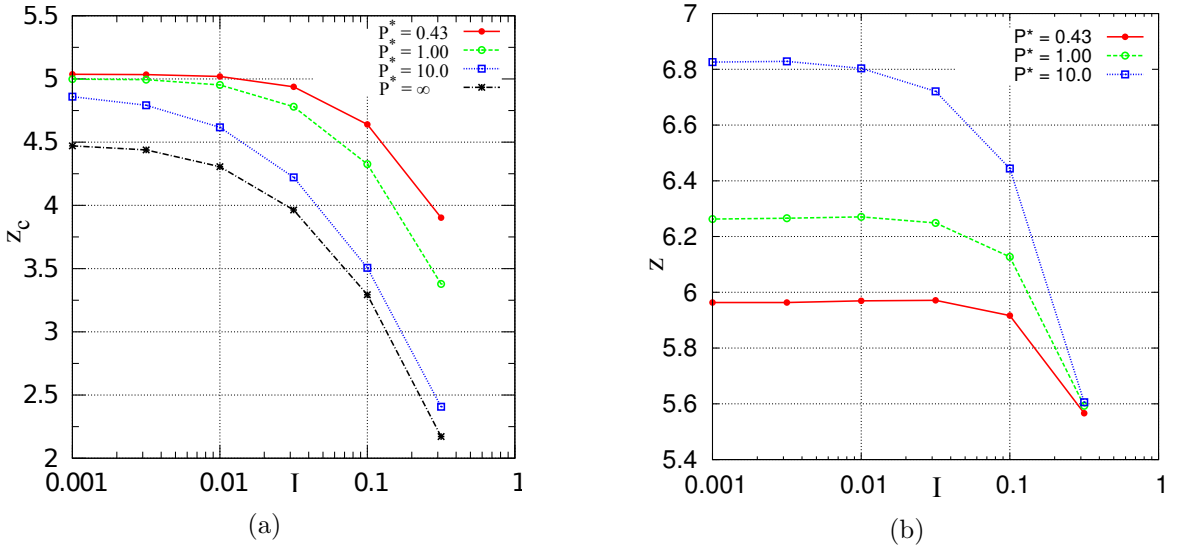

(a) (b)

FIGURE 3 – Coordination number for pairs in contact z_c (a) and for all interactions z (b) versus inertial number I for different values of P^* with rupture distance $D_0/a = 0.1$.

z decreases for larger values of I that correspond to lower solid fractions. Fig. 3b plots the contact coordination number z_c. z_c increases for lower values of P^* , but already strongly departs from its value in the dry case at quite large P^*, especially near the quasistatic limit. Enduring liquid bridges prevent contacting grains from moving apart, and, for small I, grains are at least contacting two neighbors in cohesive systems, while a significant proportion ($> 6\%$) are "rattlers" (no force-carrying contact) without cohesion.

Contact coordination number z_c is therefore, not systematically increasing with density, which is larger for smaller cohesive forces. However, the coordination number associated to close neighbors, separated by a gap smaller than h, as shown in Fig. 4, is directly correlated to ϕ for $h/a > 2.5 \times 10^{-3}$. This function is described by power law $z(h) - z(0) \propto (\frac{h}{a})^{0.6}$ in range $0 < h/a < 0.06$. On comparing $z_d = z - z_c$ (Figs. 3a, 3b) to $z(D_0)$ (Fig. 4), one deduces the proportion $x_M = \frac{z_d}{z(D_0)-z_c}$ of pairs at distance lower than D_0 joined by a meniscus : x_M varies between 0.61 and 0.68 as I increases from 10^{-3} to $10^{-0.5}$, similar to some experimental results [10].

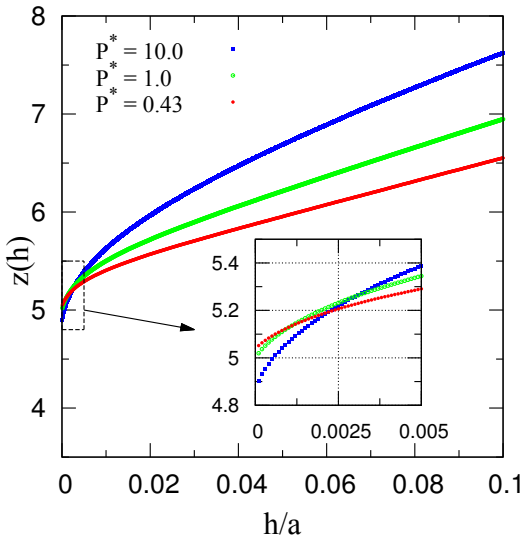

FIGURE 4 – Coordination number of close neighbors for $I = 10^{-3}$, growing with gap thickness (distance) h. Blown-up detail corresponds to small h range.

4.2 Agglomeration

As observed and reported in [4, 5], adhesive forces entail particle agglomeration, and grains that stick to one another form clusters that are transported by the flow for some distance before they are broken or restructured. As a consequence, the distribution of the age τ_c of contacts, as shown in Fig. 5, is such strain intervals $\dot{\gamma}\tau_c$) reach values of several units. This suggests that contacting pairs survive full tumbling motion in the average flow (Fig. 6). The average contact age increases as P^* decreases, indicating stronger cohesion effects produce longer lasting contacts. Little difference is noted between $I = 0.1$ and 0.01, showing little microstructural or geometric changes take place in this interval, which is not far from the quasistatic limit.

4.3 Fabric

Macroscopic friction is related to fabric anisotropy [11]. The distribution of unit vectors $\vec{n}$ normal to the surface of interacting grains can be expressed [11] with a few spherical harmonics terms and fabric parameters F_{12}, $(F_{11} - F_{22})$, $(F_{33} - 1/3)$, F_{13} and F_{23}, defined, as usual, as :

$$F_{\alpha\beta} = \langle n_\alpha n_\beta \rangle \tag{2}$$

Figs. 7a and 7b plot the fabric parameters for contact and distant interactions. In both cases F_{13} and F_{23} are negligible. $(F^c_{11} - F^c_{22})$ and $(F^c_{33} - 1/3)$ are also small. The most noteworthy contributions to

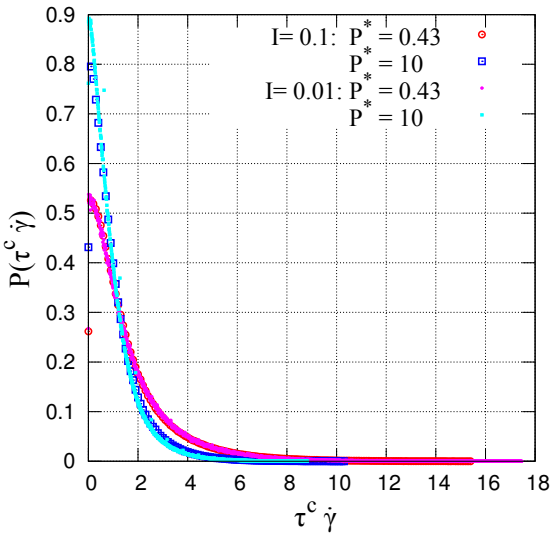

FIGURE 5 – Distribution of age of contacts $P(\tau^c\dot{\gamma})$ for two different I and P^*. Age of contacts τ^c is normalized by shearing time $1/\dot{\gamma}$.

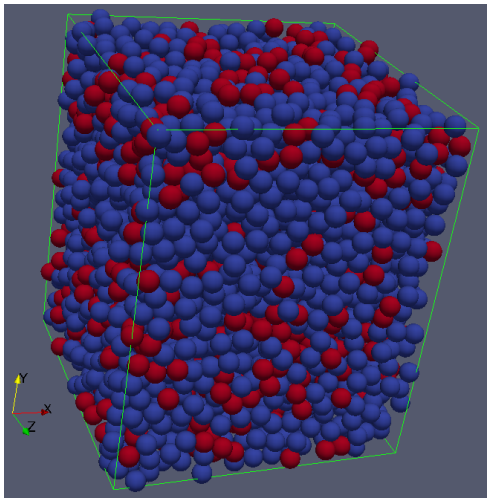

FIGURE 6 – Configuration of a system of particles in steady shear flow with $I = 0.01$ and $P^* = 0.43$. All particles that have at least one contact with $\tau^c\dot{\gamma} \geq 5$ are represented by a red color.

shear stress at small I are associated to the additive effect of contacting pairs with φ near $3\pi/4$, with $F^c_{12} = -0.03$, mostly carrying repulsive forces, on the one hand ; and of distant attractive interactions, oriented near $\varphi = \pi/4$, with $F^d_{12} = 0.14$, on the other hand. As sketched in Fig. 8, those repulsive and attractive contributions respectively correspond to approaching and receding pairs according to the average flow kinematics. This specific fabric anisotropy of distant interactions thus explains, to some extent, the important influence of the attractive forces of finite range to the material rheology.

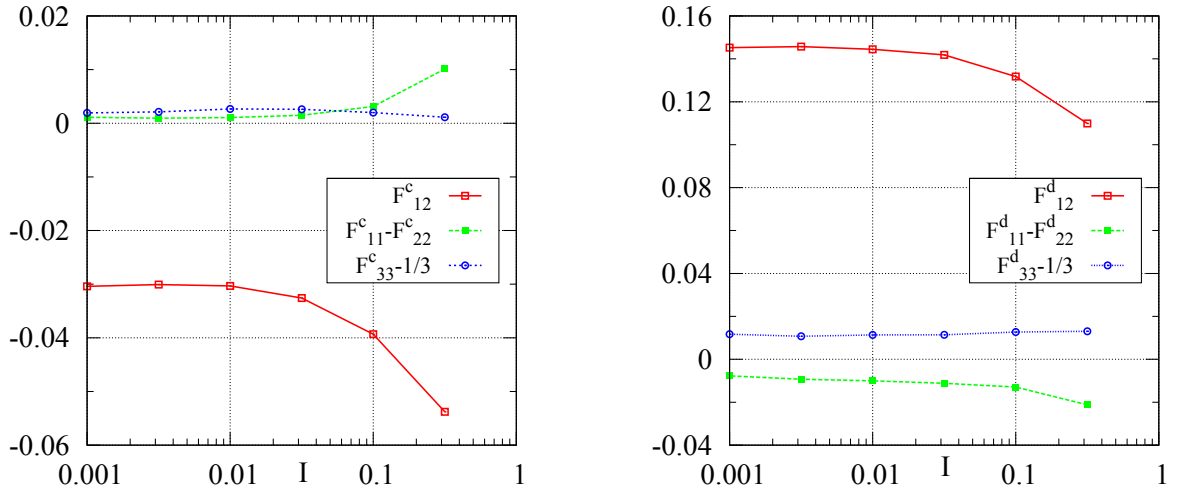

FIGURE 7 – Fabric parameters of contact interactions (a) and distant interactions (b) versus I for $P^* = 0.43$

5 Conclusions

Quantitative measurements of the rheological properties of model wet granular materials at low saturation thus reveal an important, unexpected influence of distant attractive force on the behavior. Many other features should be exploited (such as normal stress differences, related to non-negligible values of $(F^d_{11} - F^d_{22})$ and $(F^d_{33} - 1/3)$. Further studies, extending to larger saturations should reveal a

rich landscape of interesting rheophysical properties.

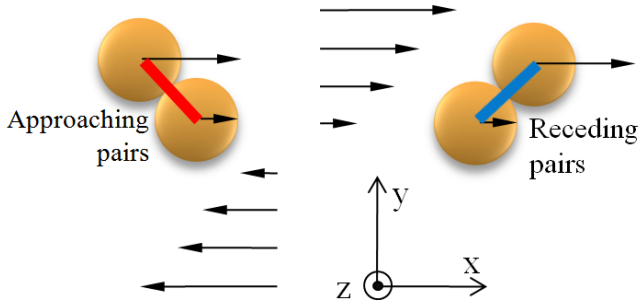

FIGURE 8 – Sketch of approaching (φ near $3\pi/4$) and receding (φ near $\pi/4$) grain pairs in shear flow.

Références

[1] Forterre, Y., Pouliquen, O. 2008 Flows of Dense Granular Media. *Annu. Rev. Fluid Mech.* **40**, 1-24.

[2] Hatano, T. 2007 Power-law friction in closely packed granular materials. *Phys. Rev. E* **75**, 060301(R).

[3] Peyneau, P. -E., Roux, J.-N. 2008 Frictionless bead packs have macroscopic friction, but no dilatancy. *Phys. Rev. E* **78**, 011307.

[4] Gilabert, F. A., Roux, J.-N., Castellanos, A. 2007 Computer simulation of model cohesive powders : Influence of assembling procedure and contact laws on low consolidation states. *Phys. Rev. E* **75**, 011303.

[5] Rognon, P. G., Roux, J.-N., Naaïm, M., Chevoir, F. 2008 Dense flows of cohesive granular materials. *J. Fluid Mech.* **596**, 21-47.

[6] Agnolin, I., Roux, J.-N. 2007 Internal states of model isotropic granular packings. I. Assembling process, geometry, and contact networks *Phys. Rev. E* **76**, 061302.

[7] Pitois, O., Moucheront, P., Chateau, X. 2000 Liquid Bridge between Two Moving Spheres : An Experimental Study of Viscosity Effects. *Journal of colloid and interface science* **231**, 26-31.

[8] Mitarai, N., Nori, F. 2006 Wet granular materials. *Advances in Physics* **55**, Nos. 1-2, 1-45.

[9] Richefeu, V., Radjaï, F., El Youssoufi, M. S. 2006 Stress transmission in wet granular materials. *Eur. Phys. J. E* **21**, 359-369.

[10] Herminghaus, S. 2005 Dynamics of wet granular matter. *Advances in Physics* **54**, No. 3, 221-261.

[11] Peyneau, P. -E., Roux, J.-N. 2008 Solidlike behavior and anisotropy in rigid frictionless bead assemblies. *Phys. Rev. E* **78**, 041307.